Nanoscale Res Lett (2009) 4:313–320
DOI 10.1007/s11671-008-9244-z

NANO EXPRESS

Two-Functional Direct Current Sputtered Silver-Containing Titanium Dioxide Thin Films

J. Musil · M. Louda · R. Cerstvy · P. Baroch · I. B. Ditta · A. Steele · H. A. Foster

Received: 23 October 2008 / Accepted: 30 December 2008 / Published online: 27 January 2009

Abstract The article reports on structure, mechanical, optical, photocatalytic and biocidal properties of Ti–Ag–O films. The Ti–Ag–O films were reactively sputter-deposited from a composed Ti/Ag target at different partial pressures of oxygen p_{O_2} on unheated glass substrate held on floating potential U_{fl}. It was found that addition of ~2 at.% of Ag into TiO_2 film has no negative influence on UV-induced hydrophilicity of TiO_2 film. Thick (~1,500 nm) TiO_2/Ag films containing (200) anatase phase exhibit the best hydrophilicity with water droplet contact angle (WDCA) lower than 10° after UV irradiation for 20 min. Thick (~1,500 nm) TiO_2/Ag films exhibited a better UV-induced hydrophilicity compared to that of thinner (~700 nm) TiO2/Ag films. Further it was found that hydrophilic TiO_2/Ag films exhibit a strong biocidal effect under both the visible light and the UV irradiation with 100% killing efficiency of *Escherichia coli* ATCC 10536 after UV irradiation for 20 min. Reported results show that single layer of TiO_2 with Ag distributed in its whole volume exhibits, after UV irradiation, simultaneously two functions: (1) excellent hydrophilicity with WDCA < 10° and (2) strong power to kill *E. coli* even under visible light due to direct toxicity of Ag.

Keywords TiO_2 · Ag addition · Mechanical properties · Hydrophilicity · Biocidal activity · Sputtering

J. Musil (✉) · M. Louda · R. Cerstvy · P. Baroch
Department of Physics, Faculty of Applied Sciences, University of West Bohemia, Univerzitní 22, 306-14 Plzeň, Czech Republic
e-mail: musil@kfy.zcu.cz

I. B. Ditta · A. Steele · H. A. Foster
Biomedical Sciences Research Institute, University of Salford, Salford M5 4WT, UK

Introduction

In recent years, a considerable attention was devoted to the development of transparent, anatase TiO_2 thin films with strong hydrophilicity induced by UV light irradiation with the aim to use them in self-cleaning, antifogging and biocidal (self-disinfection) applications [1, 2]. In view of a potential industrial utilization of the photocatalytic anatase TiO_2 thin films, the investigation was concentrated mainly on solution of three problems: (1) high-rate deposition with deposition rate $a_D \geq 50$ nm/min (economically acceptable production), (2) low-temperature deposition at temperatures ≤150 °C down to ~100 °C (to allow deposition on heat sensitive substrates such as polymer foils, polycarbonate, etc.) [3, 4 and references therein] and (3) photocatalytic TiO_2-based thin films operating under visible (vis) light irradiation (to increase the efficiency of photocatalyst in the visible region with the aim to avoid the need for irradiation with special UV lamps). In spite of a great effort, the last problem has not yet been overcome. The solution to this problem requires an increase in the absorption of visible light by the TiO_2 and thus decrease the optical band gap E_g. There have been many attempts to shift the photocatalytic function of TiO_2 films from UV to visible light by addition of different elements into TiO_2 films [5–8].

The addition of elements into TiO_2, often called "doping" of TiO_2 with carefully selected elements, has also been successfully used for improvement of UV-induced photocatalytic activity of TiO_2-based thin films [9–21]. Such films after UV irradiation exhibit the following UV-induced functions: (1) self-cleaning, (2) photodecomposition of organic compounds and (3) self-disinfection. The following elements Ag [10, 11, 19–21], Cu [13], Sb [12] were incorporated into TiO_2 film with the aim to improve

UV-induced biocidal function. Ag was not actually integrated into the bulk of TiO_2 film but only as a sublayer or a thin top layer [20]. Preliminary experiments indicated that a more compact and maybe a more efficient biocidal film could be Ag-containing TiO_2 film with Ag homogeneously distributed through the whole bulk of TiO_2 film. Therefore, the subject of this article is the formation of Ag-containing TiO_2 films with the aim to investigate the effect of Ag addition on its physical and photocatalytic properties, and biocidal activity. The effect of Ag on mechanical properties of TiO_2/Ag film is also reported.

Experimental Details

Ti–Ag–O films were reactively sputter-deposited in $Ar + O_2$ sputtering gas mixture using an unbalanced magnetron equipped with (i) composed Ti/Ag target of diameter 100 mm and (ii) NdFeB magnets. The composed target consists of Ti plate with Ag and Ti fixing ring, see Fig. 1. The amount of Ag incorporated in Ti–Ag–O film was set by the inner diameter of the Ti fixing ring. The amount of Ag incorporated into TiO_2 film almost does not depend on partial pressure of oxygen p_{O_2} used in reactive sputter-deposition of TiO_x films. In all Ti–Ag–O films described in this article, the amount of Ag was $\sim$2 at.%.

Films were sputter-deposited under the following conditions: magnetron discharge current $I_d = 2$ A, substrate bias $U_s = U_{fl}$, substrate-to-target distance $d_{s-t} = 120$ mm, partial pressure of oxygen ranging from 0 to 1.5 Pa, and total pressure of sputtering gas mixture $p_T = p_{Ar} + p_{O_2} = 1.5$ Pa;

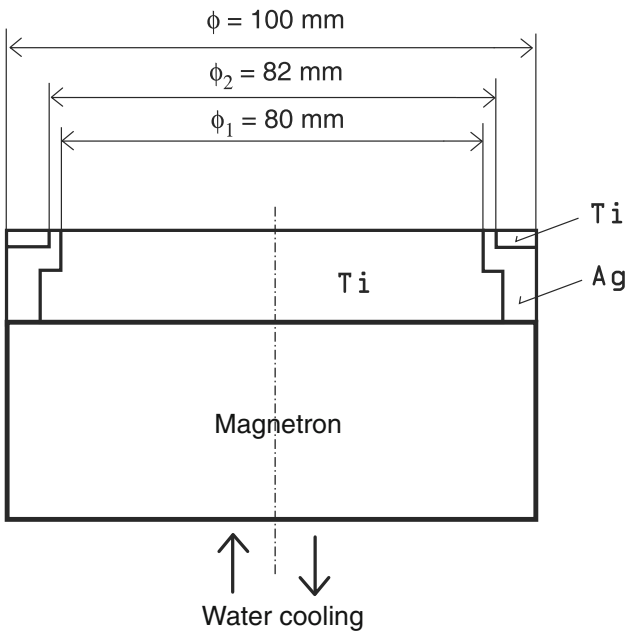

Fig. 1 Schematic of composed Ti/Ag magnetron target

U_{fl} is the floating potential. Films were deposited on unheated glass substrates ($20 \times 10 \times 1$ mm^3). The thickness h of Ti–Ag–O films ranged from $\sim$500 to 2,800 nm.

The thickness of Ti–Ag–O films was measured by a stylus profilometer DEKTAK 8 with a resolution of 1 nm. The structure of film was determined by PANalytical X'Pert PRO diffractometer working in Bragg–Bretano geometry using a Cu Kα (40 kV, 40 mA) radiation. The water droplet contact angle (WDCA) on the surface of the TiO_2 film after its irradiation by UV light (Philips TL-DK 30W/05, $W_{ir} = 0.9$ mW/cm^2 at wavelength $\lambda = 365$ nm) was measured by a Surface Energy Evaluation System made at the Masaryk University in Brno, Czech Republic. The film surface morphology was characterized by an atomic force microscopy (AFM) using AFM-Metris-2000 (Burleigh Instruments, USA) equipped with an Si_3N_4 probe. The surface and cross-section film morphology was characterized by SEM Quanta 200 (FEI, USA) with a resolution of 3.5 nm at 30 kV.

The bioactivity of Ti–Ag–O film was determined using a modified standard test described by BS:EN 13697:2001 [22]. Coated samples were shaken in 100% methanol for 40 min. Samples were removed aseptically and placed in a UVA transparent disposable plastic Petri dish, film side uppermost. The coated samples were then pre-irradiated by placing those under 3×15 W UVA bulbs with a 2.24 mW/cm^2 output for 24 h.

Escherichia coli ATCC 10536 was subcultured into nutrient broth (Oxoid, Basingstoke, UK) and inoculated onto cryobank beads (Mast Diagnostics, Liverpool, UK) and stored at −70 °C. Beads were subcultured onto nutrient agar (Oxoid) and incubated at 37 °C for 24 h and stored at 5 °C. A 50 µl loopful was inoculated into 20 ml nutrient broth and incubated for 24 h at 37 °C. Cultures were centrifuged at $5{,}000 \times$ g for 10 min in a bench centrifuge, and the cells were washed in de-ionised water three times by centrifugation and re-suspension. Cultures were re-suspended in water and adjusted to OD 0.5 at 600 nm in a spectrometer (Camspec, M330, Cambridge, UK) to give $\sim 2 \times 10^8$ colony forming units (cfu) ml^{-1}. Fifty microlitre of this suspension was inoculated on to each test sample and spread out using the edge of a flame sterilized microscope cover slip.

The prepared samples were then UV activated. Four samples were exposed to three 15 W UVA lamps at 2.29 mW/cm^2. At time zero, a sample was removed immediately and the remaining samples removed at regular intervals. Four samples exposed to UVA but covered with a polylaminar UVA protection film (Anglia Window Film, UK) to block UVA but not infra-red, acted as controls. The samples were then immersed in 20 ml of sterile de-ionised water and vortexed for 60 s to re-suspend the bacteria. A viability count was performed by serial dilution and plating

onto nutrient agar in triplicate and incubation at 37 °C for 48 h. Each experiment was performed in triplicate.

Results and Discussion

Deposition Rate

The deposition rate a_D of Ti–Ag–O film reactively sputter-deposited in a mixture of $Ar + O_2$ decreases with increasing partial pressure of oxygen p_{O_2}. It is the lowest in the oxide mode of sputtering. Under conditions used in our experiment, the deposition rate a_D of TiO_2/Ag films formed in the oxide mode is $\sim$4.5 nm/min (see Fig. 2).

Structure

Effect of Partial Pressure of Oxygen

The structure of Ti–Ag–O film strongly depends on the partial pressure of oxygen p_{O_2}. An evolution of XRD patterns from sputter-deposited thin Ti–Ag–O films with increasing p_{O_2} is displayed in Fig. 3. The change in the structure of film is connected with increasing energy delivered to it during growth mainly by bombarding ions with increasing p_{O_2} due to decrease of a_D (see Fig. 2). It follows from the formula of energy E_{bi} delivered to the unit volume of growing film by bombarding ions: $E_{bi} = E_i/e(i_s/a_D) = (U_p - U_{fl})i_s/a_D$ [4, 23]; here E_i is the energy of ion incident on a floating substrate, e is the electron charge, U_p and U_{fl} are the plasma and floating potential of substrate, respectively. In our experiment, under the assumption of zero collisions the energy $E_i \approx 30$ eV because $U_p \approx +20$ V and $U_{fl} \approx -10$ V.

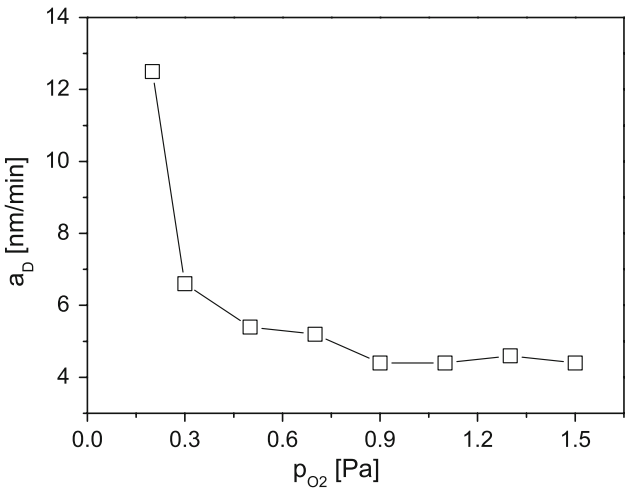

Fig. 2 Deposition rate a_D of reactively sputter-deposited Ti–Ag–O films as a function of p_{O_2}. Deposition conditions: $I_D = 2$ A, $U_S = U_{fl}$, $d_{s-t} = 120$ mm, $p_T = 1.5$ Pa

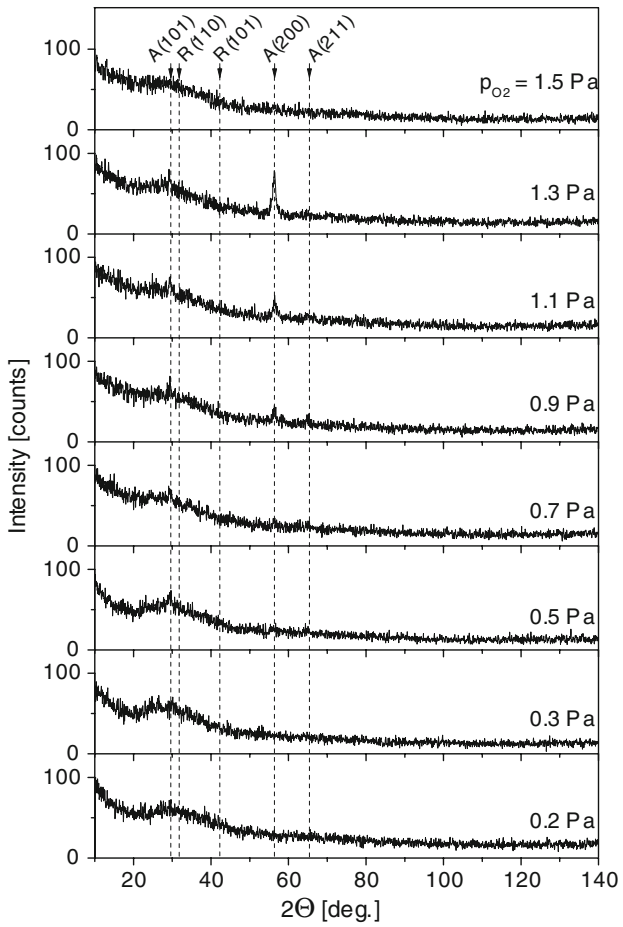

Fig. 3 XRD patterns from $\sim$500 to 700 nm thick Ti–Ag–O films sputter-deposited at $I_D = 2$ A, $U_S = U_{fl}$, $d_{s-t} = 120$ mm on unheated glass substrate, as a function of p_{O_2}

Therefore, at the end of transition mode of sputtering dominated by relatively high values of $a_D \geq 6.6$ nm/min at $p_{O_2} < 0.3$ Pa, relatively low energies E_{bi} are delivered to the growing film. It results in the formation of amorphous Ti–Ag–O films at $p_{O_2} < 0.3$ Pa. As the film deposition rate a_D decreases more energy is delivered to the growing film and the Ti–Ag–O films crystallize.

A nanocrystallization of Ti–Ag–O film, characterized by low-intensity X-ray reflections from the anatase phase, is observed at $a_D \leq 5.5$ nm/min. The nanocrystallization occurs as a consequence of longer deposition time t_d needed to form Ti–Ag–O film with the same thickness h at low values of a_D. It indicates that the film nanocrystallization was very probably due to a higher total energy $E_T = E_{bi} + E_{ca} + E_{ch}$ delivered to the growing film in the oxide mode compared to that delivered to the film sputter-deposited at higher values of a_D in the transition and metallic ($p_{O_2} \rightarrow 0$) modes of sputtering; $E_{ca}(p_T)$ and $E_{ch}(p_{O_2})$ are the energy delivered to the film by fast condensing atoms and by the heat evolved in the formation of

oxide (exothermic reaction), respectively. From Fig. 3, it is seen that the crystallinity of Ti–Ag–O film improves with increasing p_{O_2}; compare films of the same thickness $h = 600$ nm sputter-deposited at $p_{O_2} = 0.9$, 1.1 and 1.3 Pa. Because a_D of the film is almost constant for p_{O_2} ranging from 0.9 to 1.3 Pa, this experiment indicates that a main component of energy E_T delivered to the growing film is probably E_{ch}, i.e. the heat evolved in formation of the oxide. The nanocrystalline Ti–Ag–O films exhibit the anatase structure with A(200) preferred crystallographic orientation. The development of WDCA and optical band gap E_g of Ti–Ag–O films with increasing partial pressure of oxygen p_{O_2} is shown in Table 1. Surface morphology and film cross-section of thick Ti–Ag–O film prepared at $p_{O_2} = 0.5$ Pa are shown in Fig. 4. It can be seen that dense featureless structure with relatively smooth surface is developed.

The nanocrystallization of anatase phase strongly improves the hydrophilicity of the surface of Ti–Ag–O film after its UV irradiation. Almost all films sputter-deposited at $p_{O_2} \geq 0.5$ to Pa exhibit superhydrophilicity (see Table 2). The Ti–Ag–O film sputter-deposited in a pure oxygen, i.e. at $p_{O_2} = 1.5$ Pa, exhibits an X-ray amorphous structure. In spite of this fact also this film is still quite well hydrophilic.

Effect of Film Thickness

The crystallinity of TiO_2 films improved not only with increasing p_{O_2} but also with increasing film thickness h (see Fig. 5). From this figure, it can be seen that thick ($\sim$1,500 nm) films exhibited better crystallinity compared to thin ($\sim$700 nm) films sputter-deposited at the same value of p_{O_2}. It is due to a longer deposition time t_d, which enables to deliver a higher total energy E_T to the growing film at the same deposition rate a_D. More details on the evolution of intensities of XRD pattern from sputter-deposited TiO_2 films are given in the reference [3]. Thicker TiO_2/Ag films also exhibited (i) a better UV-induced hydrophilicity, (ii) lower values of the optical band gap E_g and (iii) higher roughness of the films (see Table 2 and Fig. 6, respectively). The decrease of E_g of TiO_2 film with increasing crystallinity is in agreement with our previous results [3, 4]. The anatase TiO_2 films with A(200) preferred crystallographic orientation exhibit the best hydrophilicity (see Table 2). The hydrophilicity of TiO_2/Ag, characterized with WDCA after UV irradiation, is fully comparable with that of pure TiO_2 film which exhibits WDCA of $\sim$10° or less, see for instance [3, 4, 25].

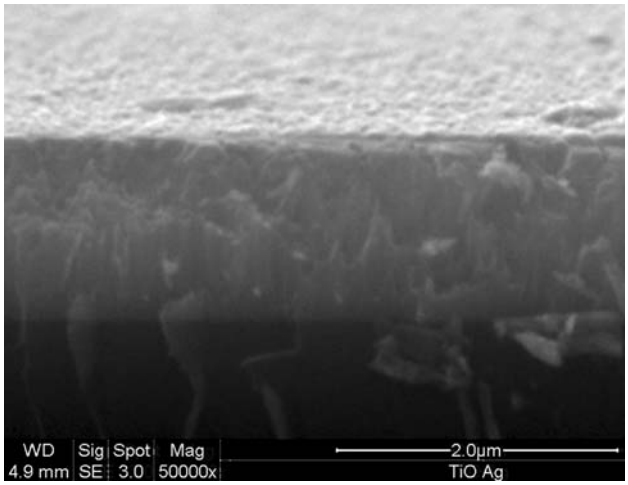

Fig. 4 Cross-section SEM image of thick ($\sim$1,500 nm) Ti–Ag–O film sputter-deposited on unheated substrate at $I_D = 2$ A, $U_S = U_{fl}$, $d_{s-t} = 120$ mm, $p_T = 1.5$ Pa and $p_{O_2} = 0.5$ Pa

Hydrophilicity of Transparent TiO_2/Ag Films

The hydrophilicity is characterized by a WDCA on the surface of TiO_2/Ag film. The development of WDCA in thin ($\sim$700 nm) and thick ($\sim$1,500 nm) TiO_2/Ag films, sputter-deposited in the oxide mode of sputtering, before and after UV irradiation with increasing p_{O_2} is displayed in Fig. 7. From this figure, it is clearly seen that a short (20 min) time of UV irradiation was sufficient to induce

Table 1 Deposition rate a_D, thickness h, WDCA after UV irradiation for 20, 60 and 300 min and optical band gap E_g of $\sim$500–700 nm thick TiO_2 films reactively sputter-deposited at $I_d = 2$ A, $p_T = 1.5$ Pa, $U_s = U_{fl}$ on unheated glass substrate as a function of partial pressure of oxygen p_{O_2}

E_g was determined using the formula given in [24]

p_{O_2} (Pa)	h (nm)	a_D (nm/min)	WDCA (°) after UV irradiation for			E_g (eV)
			20 min	60 min	300 min	
0.2	600	12.5	89	84	71	–
0.3	700	6.6	38	18	11	3.21
0.5	600	5.4	15	13	13	3.21
0.7	700	5.2	19	12	8	3.19
0.9	600	4.4	20	16	11	3.11
1.1	600	4.4	16	13	9	3.12
1.3	600	4.6	22	16	11	3.06
1.5	500	4.4	23	14	8	3.11

Table 2 Deposition rate a_D, thickness h, WDCA after UV irradiation and optical band gap E_g of thin (~500 nm) and thick (~1,500 nm) TiO_2 films reactively sputter-deposited at $I_d = 2$ A, $p_T = 1.5$ Pa, $U_s = U_{fl}$ on unheated glass substrate

p_{O_2} (Pa)	Thin films						Thick films					
	h (nm)	a_D (nm/min)	WDCA after UV irradiation			E_g (eV)	h (nm)	a_D (nm/min)	WDCA after UV irradiation			E_g (eV)
			20 min	60 min	300 min				20 min	60 min	300 min	
0.3	700	6.6	38	18	11	3.21	1,500	6.3	18	11	8	3.06
0.7	700	5.2	19	12	8	3.19	1,200	5.8	10	9	9	3.04
0.9	600	4.4	20	16	11	3.11	1,500	5.2	8	9	8	2.86

E_g was determined using the formula given in [24]

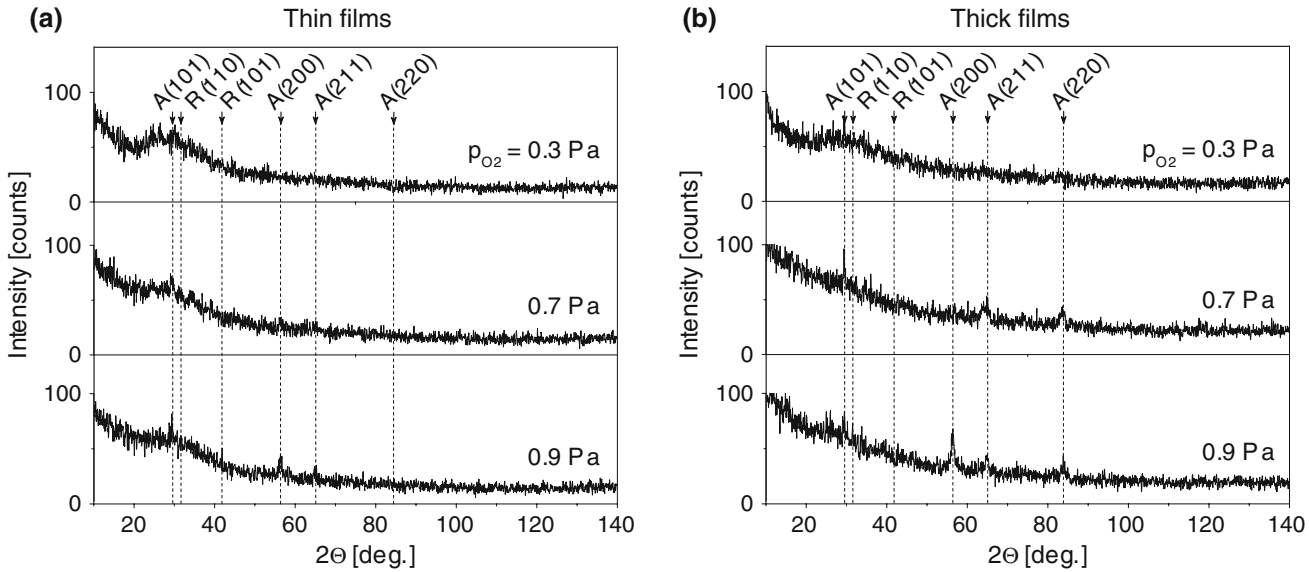

Fig. 5 Comparison of X-ray structure of **a** thin (~700 nm) and **b** thick (~1,500 nm) Ti–Ag–O films sputter-deposited on unheated glass substrate at $I_D = 2$ A, $U_S = U_{fl}$, $d_{s-t} = 120$ mm, $p_T = 1.5$ Pa and three values of $p_{O_2} = 0.3$, 0.7 and 0.9 Pa

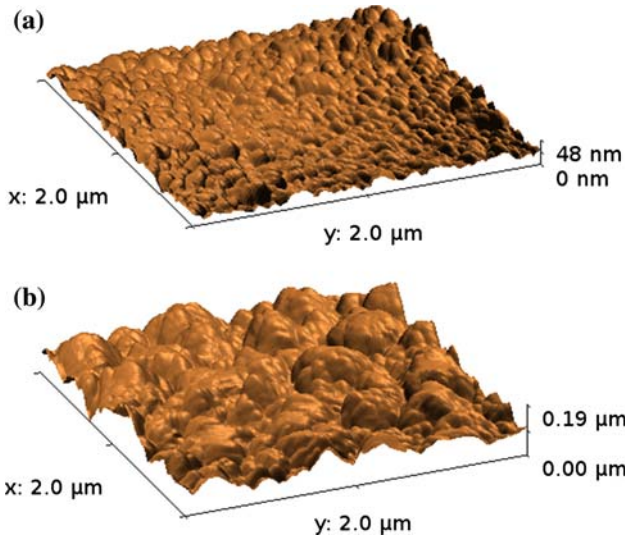

Fig. 6 Comparison of AFM surface topography of **a** thin (~700 nm) and **b** thick (~1,500 nm) Ti–Ag–O films sputter-deposited on unheated glass substrate at $I_D = 2$ A, $U_S = U_{fl}$, $d_{s-t} = 120$ mm, $p_T = 1.5$ Pa and $p_{O_2} = 0.9$ Pa

high hydrophilicity. The WDCA decreased below 10° in thick (~1,500 nm) films.

UV–Vis Transmission Spectra and Optical Band Gap of TiO_2/Ag Films

Ultraviolet–visible (UV–vis) light transmission spectra were measured on the TiO_2/Ag films sputter-deposited in the oxide mode on unheated glass substrates. The transmission spectra were measured for thin (~700 nm) and thick (~1,500 nm) TiO_2/Ag films (see Fig. 8). Thicker films exhibit a decrease in the transmission of incident light and clear shift of the absorption to higher wavelengths λ. As expected, this fact results in the decrease of (i) the optical band gap E_g and (ii) WDCA of thicker films (see Table 2 and Fig. 7). In spite of a stronger absorption of light at $\lambda = 550$ nm in thicker films, the reactively sputter-deposited TiO_2/Ag films with thickness $h \approx 1{,}500$ nm still remain semitransparent.

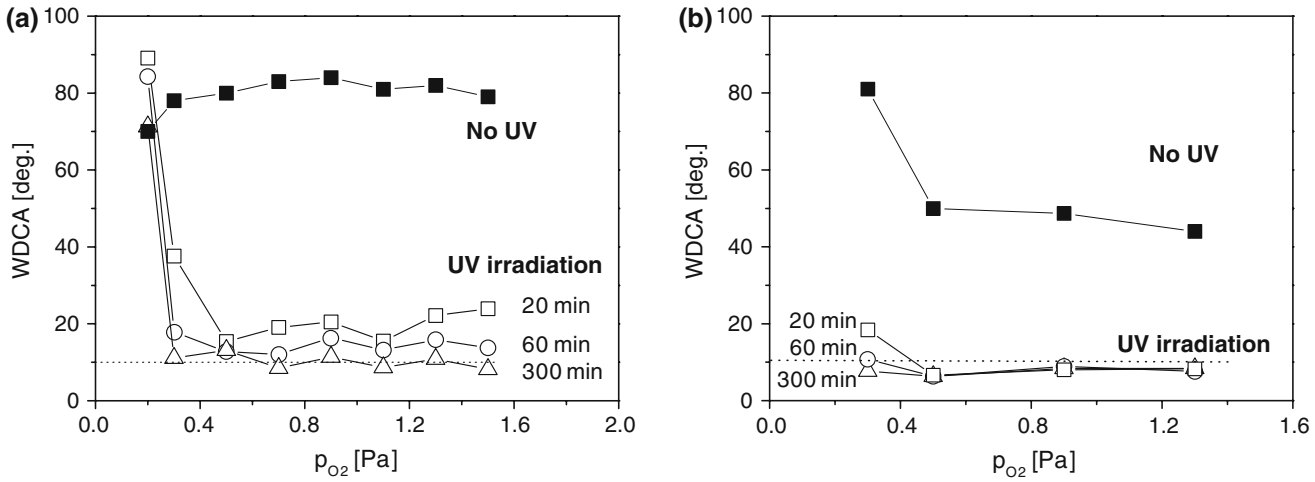

Fig. 7 Characterization of water droplet contact angle WDCA on the surface of **a** thin (~700 nm) and **b** thick (~1,500 nm) Ti–Ag–O films under UV irradiation for 20, 60 and 300 min as a function of partial pressure of oxygen p_{O_2}. Deposition conditions: $I_D = 2$ A, $U_S = U_{fl}$, $d_{s-t} = 120$ mm, unheated glass substrate

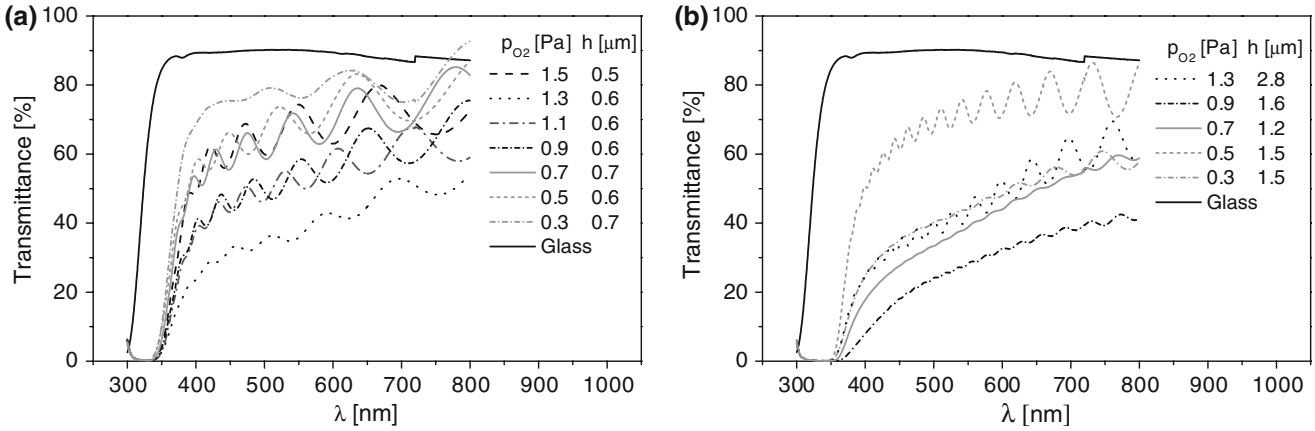

Fig. 8 Transmission spectra of **a** thin (~700 nm) and **b** thick (~1,500 nm) Ti–Ag–O films sputter-deposited on unheated substrates as a function of p_{O_2}. Deposition conditions: $I_D = 2$ A, $U_S = U_{fl}$, $d_{s-t} = 120$ mm

Also, it is worthwhile to note that in spite of the decrease of E_g and the shift of the absorption of electromagnetic waves into visible region, the hydrophilicity of surface of Ti–Ag–O film must be induced by UV light (see Fig. 7). A very short (≤20 min) UV irradiation time was sufficient to induce hydrophilicity. The need for surface activation by UV, however, indicates that the decreasing of E_g and the shifting of absorption into vis region are not sufficient conditions to prepare hydrophilic TiO_2-based films under visible light. The key parameters, which affect the photo-induced hydrophilicity of TiO_2-based films under visible light are not known so far. Recent experiments performed in our laboratory indicate that the film nanostructure could be of a key importance for the creation of hydrophilic TiO_2-based films operating under visible light only, i.e. without UV irradiation.

Mechanical Properties

The microhardness H, effective Young's modulus E^* and resistance to plastic deformation, which is proportional to the ratio H^3/E^{*2} [26] were measured for ~950 nm thick Ti–Ag–O films as a function of partial pressure of oxygen p_{O_2} (see Fig. 9). All quantities vary only slightly with p_{O_2} increasing above 0.5 Pa. The values of H are low of about 4–5 GPa. The resistance to plastic deformation characterized by the ratio H^3/E^{*2} is also very low of about 0.01. The hardness H needs to be increased and it could be achieved

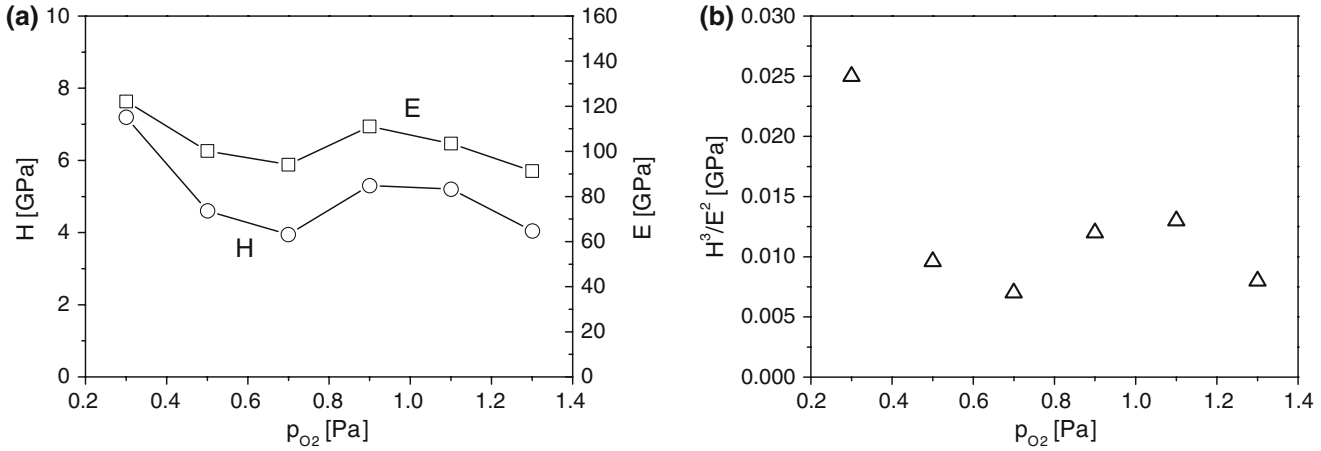

Fig. 9 **a** Microhardness H and effective Young's modulus E^* and **b** ratio H^3/E^2 of ~950 nm thick Ti–Ag–O films as a function of partial pressure of oxygen p_{O_2}. Deposition conditions: $I_D = 2$ A, $U_S = U_{fl}$, $d_{s-t} = 120$ mm

by substrate biasing. However, such experiment has not been performed so far and is the subject of our next investigations.

Antibacterial Properties

The bioactivity of Ti–Ag–O films was tested by killing the bacterium *E. coli* ATCC 10536 on the surface of 500 nm thick TiO_2/Ag single layer sputter-deposited in the oxide mode on unheated glass substrate during UV irradiation for a given time t_{ir}. The results are shown in Fig. 10. For comparison, the killing of *E. coli* bacteria on uncoated plain glass and plain glass-coated with TiO_2 layer is also given. The glass coated with TiO_2/Ag single layer exhibits the fastest killing; 20 min of UV irradiation was sufficient for 100% kill (six orders of magnitude reduction).

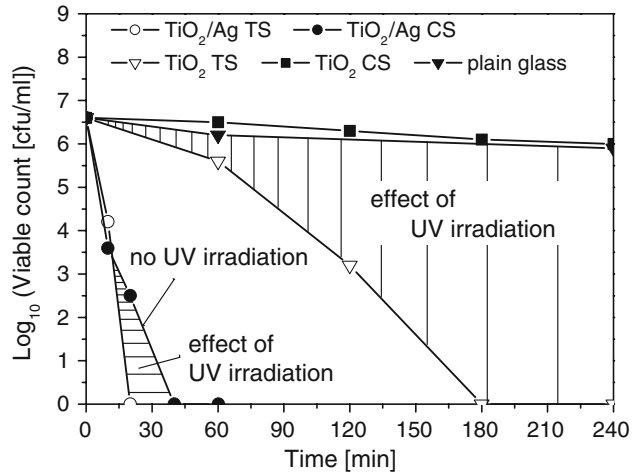

Fig. 10 Colony forming units (cfu/ml) on surface of plain glass, glass coated with TiO_2 (commercial TiO_2) with (TiO_2 TS) and without (TiO_2 CS) UV irradiation, and TiO_2/Ag single layer with (TiO_2/Ag TS) and without (TiO_2/Ag CS) UV irradiation as a function of irradiation time

Figure 10 further shows a comparison of the biocidal activity of TiO_2 and TiO_2/Ag films. There was a big difference in biocidal activity of TiO_2 test sample (TS) (irradiation under UV lamp by both UV + IR) and control TiO_2 sample (CS) (irradiated by IR only; the sample is covered with a polylaminar UVA protection film, which blocks UV from UV lamp); here IR is the infra-red radiation. A strong effect of UV irradiation on killing activity is clearly seen. The 100% kill of *E. coli* on TiO_2 surface is seen after 180 min of UV irradiation while no killing is observed on TiO_2 surface without UV irradiation after 240 min.

In contrast, 100% kill of *E. coli* on TiO_2/Ag surface is seen not only after UV irradiation (20 min) but also without UV irradiation (40 min). This result indicates that the killing of *E. coli* on TiO_2/Ag surface is probably due to a combination of direct toxicity of Ag- and UV-induced photocatalytic activity. Results shown in Fig. 10 indicate that the direct toxicity of Ag was probably dominant. The dashed areas in Fig. 10 denote the effect of UV irradiation on killing of the bacterium *E. coli* on TiO_2 and TiO_2/Ag surface.

Conclusions

The main results of investigation of physical and functional properties of sputter-deposited Ti–Ag–O thin films with low (≤2 at.%) content of Ag can be summarized as follows. TiO_2/Ag films with anatase phase and small amount (~2 at.%) of Ag exhibited an excellent UV-induced hydrophilicity. The added Ag due to strong toxicity also very rapidly killed *E. coli* on TiO_2/Ag surface. This shows that the surface of TiO_2/Ag film can be simultaneously hydrophilic and antibacterial. Therefore, crystalline

TiO_2/Ag film can be used as two-functional material. One hundred per cent kill of *E. coli* on the surface of TiO_2/Ag film was observed under *visible light* in 40 min. No UV-induced irradiation was needed. Formation of crystalline Ti–Ag–O film required a minimum total energy E_T to be delivered to the growing film. Therefore, the crystallinity of TiO_2/Ag film improves with its increasing thickness h. A longer deposition time t_d needed to form a thicker film at the same deposition rate a_D results in greater total energy E_T delivered to the growing film. Nanocrystalline TiO_2/Ag films exhibit excellent hydrophilicity ($\leq 10°$) already after a short (20 min) time of UV irradiation. Nanocrystallization of TiO_2/Ag film sputter-deposited in the oxide mode on floating unheated glass substrate ($U_s = U_{fl}$) is very probably induced by the heat evolved during formation of oxide (exothermic reaction).

Based on the results given above, the next investigation in this field should be concentrated on the physical and functional properties of nanocrystalline TiO_2-based films.

Acknowledgements This work was supported in part by the Ministry of Education of the Czech Republic under Project MSM# 4977751302, in part by Project PHOTOCOAT No. GRD1-2001-40701 funded by the European Community and in part by the Grant Agency of the Czech Republic under Project No. 106/06/0327. Authors would like to thank also to Mgr. Zdenek Stryhal, Ph.D. and Ing. Rostislav Medlin for performing AFM and SEM analysis, respectively.

References

1. N. Sakai, A. Fujishima, T. Watanabe, K. Hashimoto, J. Phys. Chem. B **107**, 1028 (2003). doi:10.1021/jp022105p
2. K. Hashimoto, H. Irie, A. Fujishima, Jpn J. Appl. Phys. **44**(Part 1), 8269 (2005). doi:10.1143/JJAP.44.8269
3. J. Musil, D. Herman, J. Sicha, J. Vac. Sci. Technol. A **24**, 521 (2006). doi:10.1116/1.2187993
4. J. Musil, J. Sicha, D. Herman, R. Cerstvy, J. Vac. Sci. Technol. A **25**(4), 666 (2007). doi:10.1116/1.2736680
5. R. Asahi, T. Morikawa, T. Ohwaki, K. Aoki, Y. Taga, Science **293**, 269 (2001). doi:10.1126/science.1061051
6. M. Anpo, M. Takeuchi, J. Catal. **216**, 505 (2003). doi:10.1016/S0021-9517(02)00104-5
7. S. Yang, L. Gao, J. Am. Ceram. Soc. **87**, 1803 (2004). doi:10.1111/j.1551-2916.2004.00733.x
8. Y.H. Tseng, C.S. Kuo, C.H. Huang, Y.Y. Li, P.W. Chou, C.L. Cheng, M.S. Wong, Nanotechnology **17**, 2490 (2006). doi:10.1088/0957-4484/17/10/009
9. C. He, Y. Xiong, X. Zhu, Thin Solid Films **422**, 235 (2002). doi:10.1016/S0040-6090(02)00892-1
10. J. Wang, J. Li, L. Ren, A. Zhao, P. Li, Y. Leng, H. Sun, N. Huang, Surf. Coat. Technol. **201**, 6893 (2007). doi:10.1016/j.surfcoat.2006.09.109
11. H.Q. Tang, H.J. Feng, J.H. Zheng, J. Zhao, Surf. Coat. Technol. **201**, 5633 (2007). doi:10.1016/j.surfcoat.2006.07.171
12. H.J. Zhang, D.Z. Wen, Surf. Coat. Technol. **201**, 5720 (2007). doi:10.1016/j.surfcoat.2006.07.109
13. X.B. Tian, Z.M. Wang, S.Q. Yang, Z.J. Luo, R.K.Y. Fu, P.K. Chu, Surf. Coat. Technol. **201**, 8606 (2007). doi:10.1016/j.surfcoat.2006.09.322
14. I.M. Arabatzis, T. Stergiopoulos, M.C. Bernard, D. Labou, S.G. Neophytides, P. Falaras, Appl. Catal. Environ. **42**, 187 (2003). doi:10.1016/S0926-3373(02)00233-3
15. F. Falaras, I.M. Arabatzis, T. Stergiopoulos, M.C. Bernard, Int. J. Photoenergy **5**, 123 (2003). doi:10.1155/S1110662X03000230
16. S.X. Liu, Z.P. Qu, X.W. Han, C.L. Sun, Catal. Today **93–95**, 877 (2004). doi:10.1016/j.cattod.2004.06.097
17. Y. Liu, C. Liu, Q. Rong, Z. Zhang, Appl. Surf. Sci. **230**, 7 (2003). doi:10.1016/S0169-4332(03)00836-5
18. Y.L. Kuo, H.W. Chen, Y. Ku, Thin Solid Films **515**, 3461 (2007). doi:10.1016/j.tsf.2006.10.085
19. M. Stir, R. Nicula, E. Burkel, J. Eur. Ceram. Soc. **26**, 1542 (2006). doi:10.1016/j.jeurceramsoc.2005.03.260
20. L.A. Brook, P. Evans, H.A. Foster, A. Steele, D.W. Sheel, H.M. Yates, J. Photochem. Photobiol. A **187**, 53 (2007). doi:10.1016/j.jphotochem.2006.09.014
21. L.A. Brook, P. Evans, H.A. Foster, M.E. Pemble, D.W. Sheel, A. Steele, H.M. Yates, Surf. Coat. Technol. **201**, 9373 (2007). doi:10.1016/j.surfcoat.2007.04.020
22. Anon, BS EN 13697:2001, Chemical disinfectants and antiseptics. Quantitative non-porous surface test for the evaluation of bacterial and/or fungicidal activity of chemical disinfectants used in food, industrial, domestic and institutional areas. Test method and requirements without mechanical action. British Standards Institute, London, 2001
23. J. Musil, J. Suna, Mater. Sci. Forum **502**, 291 (2005)
24. P.M. Kumar, S. Badrinarayanan, M. Sastry, Thin Solid Films **358**, 122 (2000). doi:10.1016/S0040-6090(99)00722-1
25. T.Y. Tsui, G.M. Pharr, W.C. Oliver, C.S. Bhatia, R.L. White, S. Anders, A. Anders, I.G. Brown, Mater. Res. Soc. Symp. Proc. **383**, 447 (1995)
26. J. Sicha, D. Herman, J. Musil, Z. Stryhal, J. Pavlik, Nanoscale Res. Lett.**2**, 123 (2007). doi:10.1007/s11671-007-9042-z